Supplementary materials for

# Realizing the Ultralow Lattice Thermal Conductivity of $Cu_3SbSe_4$ compound via Sulfur Alloying Effect

Lijun Zhao[1], Haiwei Han[1], Zhengping Lu[1], Jian Yang[2,*], Xinmeng Wu[1], Bangzhi Ge[3], Lihua Yu[1], Zhongqi Shi[4], Abdulnasser M. Karami[5], Songtao Dong[1], Shahid Hussain[2], Guanjun Qiao[2], and Junhua Xu[1,*]

[1]School of Materials Science and Engineering, Jiangsu University of Science and Technology, Zhenjiang 212100, China

[2]School of Materials Science and Engineering, Jiangsu University, Zhenjiang 212013, China

[3]State Key Laboratory of Solidification Processing, and Key Laboratory of Radiation Detection Materials and Devices, Ministry of Industry and Information Technology, Northwestern Polytechnical University, Xi'an 710072, China

[4]State Key Laboratory for Mechanical Behavior of Materials, Xi'an Jiaotong University, Xi'an 710049, China

[5]Department of Chemistry, College of Science, King Saud University, Riyadh 11451, Saudi Arabia

**Corresponding authors:*

jyyangj@ujs.edu.cn (J. Yang);

jhxu@just.edu.cn (J.H. Xu)

## Theoretical methods

### 1. Calculations of Lorenz number ($L$) and electrical thermal conductivity ($\kappa_{ele}$)

Measured $D$ for pristine $Cu_3SbSe_4$ and $Cu_3Sb(Se_{1-x}S_x)_4$ ($x$=0.1–1) samples are shown in Figure S4. The lattice thermal conductivity ($\kappa_{lat}$) is obtained by subtracting electrical thermal conductivity ($\kappa_{ele}$) from $\kappa_{tot}$ using Wiedeman-Franz relationship [1].

$$\kappa_{ele} = L\sigma T \tag{S1}$$

where $L$ is the Lorenz number and it can be expressed as equation (2) [2,3].

$$L = 1.5 + \exp\left[\frac{-|S|}{116}\right] \tag{S2}$$

The estimated Lorenz number of $Cu_3Sb(Se_{1-x}S_x)_4$ ($x$=0–1) samples are listed in Figure S5.

## Supporting figures

1. SEM, BSE and EDS spectrum of $Cu_3Sb(Se_{1-x}S_x)_4$ ($x$=0.3) sample

The four constituent elements Cu, Sb, Se and S are uniformly distributed in the selected area (marked A), and the atomic ratio (%) of Cu, Sb, Se and S is 40.07: 12.68: 31.26: 15.59 (Figure S1c), demonstrating that the formation of a solid solution of $Cu_3SbSe_4$-$Cu_3SbS_4$ ($x$=0.3), which is consistent with XRD results.

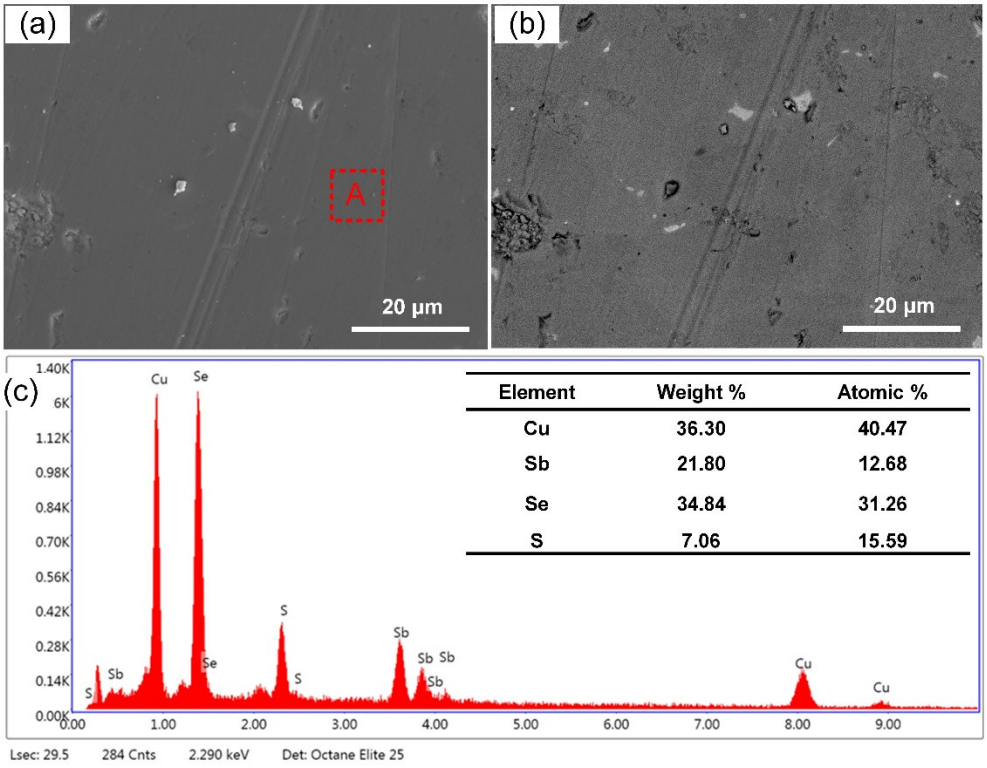


**Figure S1** (a) SEM, (b) BSE and (c) EDS spectrum of polished surface of $CuSbSe_{2.8}S_{1.2}$ sample.

2. TEM morphology and EDS mapping images of $Cu_3Sb(Se_{1-x}S_x)_4$ ($x$=0.3) sample.

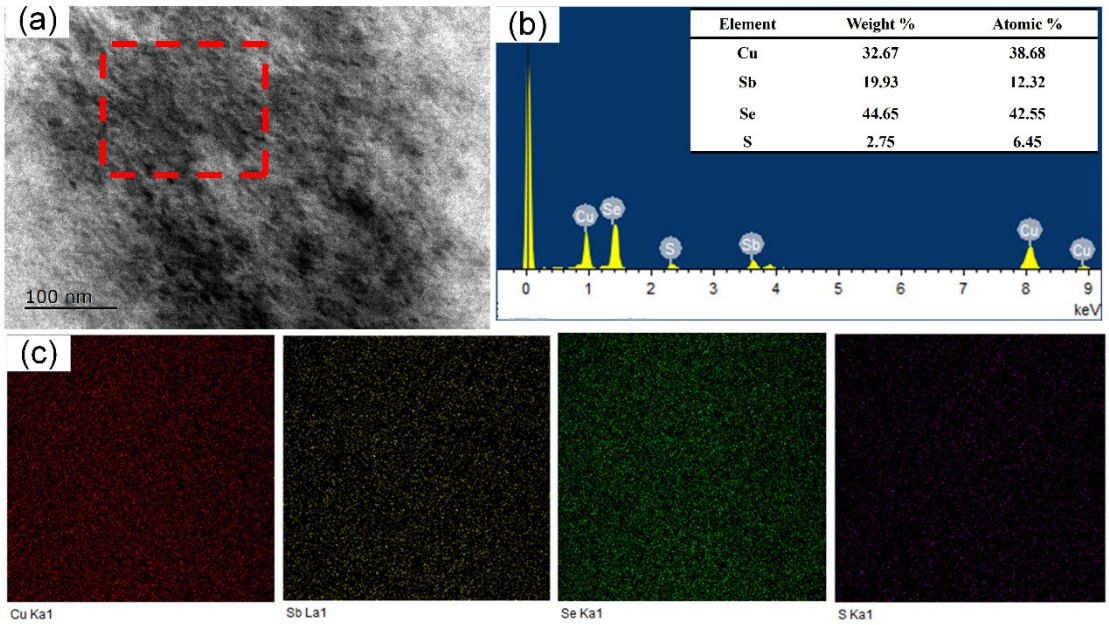


**Figure S2** TEM morphology images of $Cu_3SbSe_{2.8}S_{1.2}$ sample.

3. Band gap ($E_g$) of $Cu_3Sb(Se_{1-x}S_x)_4$ samples

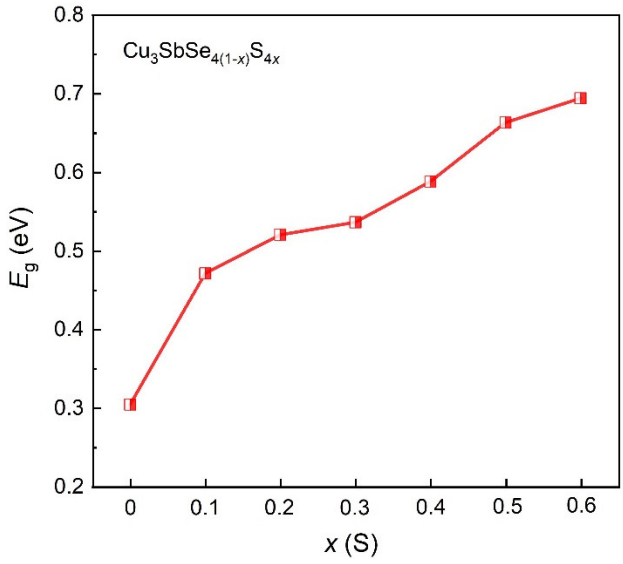


**Figure S3** Band gap ($E_g$) of $Cu_3Sb(Se_{1-x}S_x)_4$ ($x$=0–0.6) samples.

4. Measured *D*

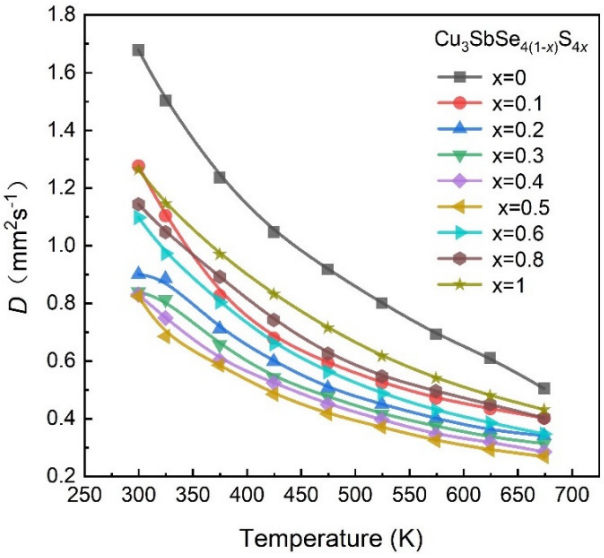


**Figure S4** Temperature-dependent *D* of $Cu_3Sb(Se_{1-x}S_x)_4$ (*x*=0–1) samples.

5. Calculated *L*

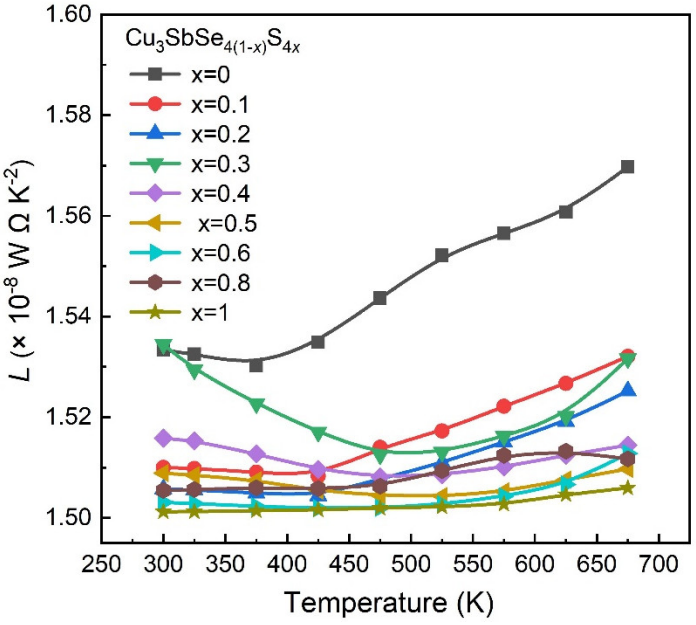


**Figure S5** Temperature-dependent Lorenz number (*L*) of $Cu_3Sb(Se_{1-x}S_x)_4$ (*x*=0–1) samples.

## Supporting table

**Table S1** Relative density, carrier concentration, Hall mobility and carrier effective mass for $Cu_3SbSe_{4(1-x)}S_{4x}$($x$=0–1) samples at room temperature (300 K)**.**

| Samples | Density （$gcm^{-3}$) | Relative density (%) | Carrier concentration ($10^{18}$ $cm^{-3}$) | Hall mobility ($cm^2$ $V^{-1}$ $s^{-1}$) | Carrier effective mass ($m_e$) |
|---|---|---|---|---|---|
| $x$=0 | 5.79 | 98.8 | 1.08 | 62.2 | 0.68 |
| $x$=0.1 | 5.53 | 94.3 | 1.55 | 24.7 | 2.48 |
| $x$=0.2 | 5.39 | 92.0 | 1.69 | 26.2 | 4.45 |
| $x$=0.3 | 5.33 | 91.0 | 6.28 | 48.6 | 2.12 |
| $x$=0.4 | 4.9 | 83.6 | 4.37 | 37.5 | 3.36 |
| $x$=0.5 | 4.72 | 80.5 | 3.35 | 35.2 | 4.77 |
| $x$=0.6 | 4.65 | 79.4 | 0.88 | 30.4 | 5.03 |
| $x$=0.8 | 4.56 | 77.8 | 0.77 | 15.1 | 2.78 |
| $x$=1 | | | 0.15 | 12.5 | 3.62 |

**Table S2** The Refined parameters and quality factors of $Cu_3SbSe_{4(1-x)}S_{4x}$ ($x$=0–1) samples.

| Nominal composition | Space group | $a$ (Å) | $c$ (Å) | $V$ (Å$^3$) | $R_p$ (%) | $R_{wp}$ (%) | $R_{exp}$ (%) | *Chi2* |
|---|---|---|---|---|---|---|---|---|
| x=0 | I$\bar{4}$2m | 5.6537 | 11.252 | 359.66 | 5.97 | 8.06 | 2.35 | 11.8 |
| x=0.1 | I$\bar{4}$2m | 5.6505 | 11.246 | 359.06 | 5.39 | 7.18 | 2.34 | 9.43 |
| x=0.2 | I$\bar{4}$2m | 5.6035 | 11.136 | 349.66 | 6.47 | 8.77 | 4.82 | 3.11 |
| x=0.3 | I$\bar{4}$2m | 5.5718 | 11.106 | 344.78 | 2.91 | 3.73 | 2.19 | 2.91 |
| x=0.4 | I$\bar{4}$2m | 5.5491 | 11.033 | 339.73 | 5.77 | 7.40 | 4.64 | 2.55 |
| x=0.5 | I$\bar{4}$2m | 5.5238 | 11.005 | 335.79 | 5.77 | 7.32 | 4.62 | 2.51 |
| x=0.6 | I$\bar{4}$2m | 5.4980 | 10.863 | 328.37 | 7.43 | 9.80 | 4.69 | 4.37 |
| x=0.8 | I$\bar{4}$2m | 5.4492 | 10.806 | 320.87 | 6.64 | 8.58 | 4.82 | 3.17 |
| x=1 | I$\bar{4}$2m | 5.3866 | 10.750 | 311.92 | 7.69 | 9.78 | 4.57 | 4.59 |

**Table S3** Parameters of $Cu_3SbSe_{4(1-x)}S_{4x}$($x$=0–1) samples obtained by fitting the experimental lattice thermal conductivity data to the Debye-Callaway model using ν=1991.2m/s, and $\theta_D$ =131K, respectively [4–6] .

| Nominal composition | $\Gamma_m$ | $\Gamma_s$ | $\Gamma$ | $u$ | $\kappa_{lat}$ ($W\,m^{-1}\,K^{-1}$) | $\kappa_{exp}$ ($W\,m^{-1}\,K^{-1}$) |
|---|---|---|---|---|---|---|
| $x$=0 | 0 | 0 | 0 | — | 3.0 | — |
| $x$=0.1 | 0.0171 | 0.0427 | 0.0597 | 1.5468 | 1.9335 | 2.015 |
| $x$=0.2 | 0.0323 | 0.0724 | 0.1047 | 2.0420 | 1.6387 | 1.636 |
| $x$=0.3 | 0.0452 | 0.0901 | 0.1353 | 2.3146 | 1.5074 | 1.521 |
| $x$=0.4 | 0.0552 | 0.0969 | 0.1521 | 2.4465 | 1.4504 | 1.514 |
| $x$=0.5 | 0.0616 | 0.0940 | 0.1556 | 2.4674 | 1.4417 | 1.373 |
| $x$=0.6 | 0.0635 | 0.0831 | 0.1466 | 2.3879 | 1.4752 | 1.707 |
| $x$=0.7 | 0.0684 | 0.0755 | 0.1438 | 2.3580 | 1.4882 | — |
| $x$=0.8 | 0.0492 | 0.0449 | 0.0941 | 1.9014 | 1.7144 | 1.880 |
| $x$=0.9 | 0.0300 | 0.0220 | 0.0520 | 1.4093 | 2.0301 | — |
| $x$=1 | 0 | 0 | 0 | — | — | — |

## References


[1] Mahan, G.; Bartkowiak, M. Wiedemann–Franz law at boundaries. Appl. Phys. Lett. **1999**, 74, 953–954.

[2] Kim, H.S.; Gibbs, Z.M.; Tang, Y.G.; Wang, H.; Snyder, G.J. Characterization of Lorenz number with Seebeck coefficient measurement. APL. Mater. **2015**, 3, 041506.

[3] Wang, B.Y.; Zheng, S.Q.; Wang, Q.; Li, Z.L.; Li, J.; Zhang, Z.P.; Wu, Y.; Zhu, B.S.; Wang, S.Y.; Chen, Y.X.; Chen, L.Q.; Chen, Z.-G. Synergistic modulation of power factor and thermal conductivity in $Cu_3SbSe_4$ towards high thermoelectric performance. Nano Energy **2020**, 71, 104658.

[4] Skoug, E.J.; Cain, J.D.; Morelli, D.T. High thermoelectric figure of merit in the $Cu_3SbSe_4$-$Cu_3SbS_4$ solid solution. Appl. Phys. Lett. **2011**, 98, 261911.

[5] Yang, J.; Meisner, G.P.; Chen, L.D. Strain field fluctuation effects on lattice thermal conductivity of ZrNiSn-based thermoelectric compounds. Appl. Phys. Lett. **2004**, 85, 1140−1142.

[6] Wan, C.L.; Pan, W.; Xu, Q.; Qin, Y.X.; Wang, J.D.; Qu, Z.X.; Fang, M.H. Effect of point defects on the thermal transport properties of $(La_xGd_{1-x})_2Zr_2O_7$: Experiment and theoretical model. Phys. Rev. B **2006**, 74, 144109.